JOURNAL OF MATERIALS SCIENCE **34** (1999) 71 – 75

Fracture behavior of hybrid platelet-fiber alumina preforms

S. CARDINAL, M. R'MILI, P. MERLE
Institut National des Sciences Appliquées de Lyon, GEMPPM, UMR CNRS 5510, 20 Avenue Albert Einstein, F 69621 Villeurbanne Cedex, France
E-mail: cardinal@gemppm.insa-lyon.fr

We studied the fracture behavior of alumina platelet preforms, with a global porosity of 80%, containing a weight fraction of short fibers varying between 0 and 50%. This addition of fibers leads to an increase in the work of fracture of the preform. An experimental method was set up to obtain a controlled rupture of these specimens and a load–displacement curve which allowed us to measure the increment of rupture energy due to the fiber pull-out. Experimental curves were interpreted by means of a micromechanical model developed initially for the study of the fracture behavior of ceramic matrix composites. This led us to estimate an equivalent friction stress between fibers and platelets of the order of 0.04 MPa.

1. Introduction
The interest in using plate-like particles to reinforce materials has been shown both by experimental studies [1–3] and theoretical considerations [4, 5]. For an identical volume fraction of reinforcement, a greater stiffness is obtained than in the case of equiaxed particles. However, preforms elaborated from these particles are brittle and fracture during high pressure infiltration. It has been demonstrated that this phenomenon could be overcome by incorporating fibers in the platelet preform [6]. The addition of short fibers, which bridge the growing crack, leads to an increase of the fracture toughness of brittle materials, by providing energy dissipation mechanisms.

The aim of this work was to find a good experimental method to study the fracture behavior of these hybrid fiber/platelet preforms. We set up an experimental device to determine the load (P)—displacement (δ) curve (P–δ curve), during the fracture process. This enabled us to evaluate the contribution of the fibers to the crack propagation resistance and to show the role played by the percentage of fibers on the pull out energy of the hybrid preform.

2. Materials
The materials used for the elaboration of preforms are hexagonal and monocrystalline α-alumina platelets, elaborated by Elf-Atochem, and Almax α-alumina short fibers. The diameter of the platelets is 10 μm, their thickness 1 μm and their density 3.97 g/cm^3. The mean length of the fibers is 0.8 mm and their mean diameter 10 μm. They are polycrystalline, with a mean grain size of the order of a micrometer and thus their density is 3.6 g/cm^3, slightly less than that of monocrystalline platelets.

The hybrid preform is prepared by mixing the alumina platelets, the alumina fibers and an organic binder in a slurry. The reinforcement (fibers and platelets) is dispersed by ultrasound and the blend is mechanically stirred to obtain a homogeneous repartition of the fibers in the platelets. The liquid in the slurry is removed by vacuum filtration to form a wet cake with a predetermined shape. This wet cake is then dried at a temperature of 100 °C, and heated at 625 °C to remove the organic binder. The mechanical properties of the obtained preform are improved by a final sintering treatment of 3 h at 1300 °C. Preforms containing a weight fraction (r_f) of fibers varying between 0 and 50% have thus been elaborated.

SEM observations show a good repartition of fibers in the hybrid preform even if their percentage is high. An example of such a distribution is shown by Fig. 1, relative to a preform with $r_f = 50\%$. The global porosity of the preforms has been determined from the weight and dimensions of the sample and is about 80% for each preform. Table I gives the results obtained for various r_f between 0 and 50%.

The pore size distribution was determined by the mercury intrusion technique. Fig. 2 gives the histogram of the mean pore size obtained on a hybrid preform with $r_f = 35\%$. This histogram exhibits a narrow peak, centered around a mean value of 9 μm, which confirms the homogeneity of the material.

3. Experimental techniques
The P–δ curve and the work of fracture were determined from uniaxial tensile tests. They were performed on samples with dimensions of $10 \times 10 \times 25$ mm^3. The samples were glued with epoxy to aluminum blocks to facilitate gripping and the system was carefully aligned to minimize bending stresses. To control the rupture,

TABLE I Final porosities of hybrid preforms

Weight percentage of fibers r_f (%)	Volume percentage of (fibers/platelets) in preform V_f (%)	Preform density (measured)	Porosity (%)
0	(0/20)	0.794 ±0.001	80.0 ±0.1
10	(2.2/18.2)	0.868 ±0.001	77.9 ±0.1
20	(4.3/15.7)	0.859 ±0.001	77.9 ±0.1
35	(7.5/12.5)	0.796 ±0.001	79.2 ±0.1
50	(10.5/9.5)	0.766 ±0.001	79.6 ±0.1

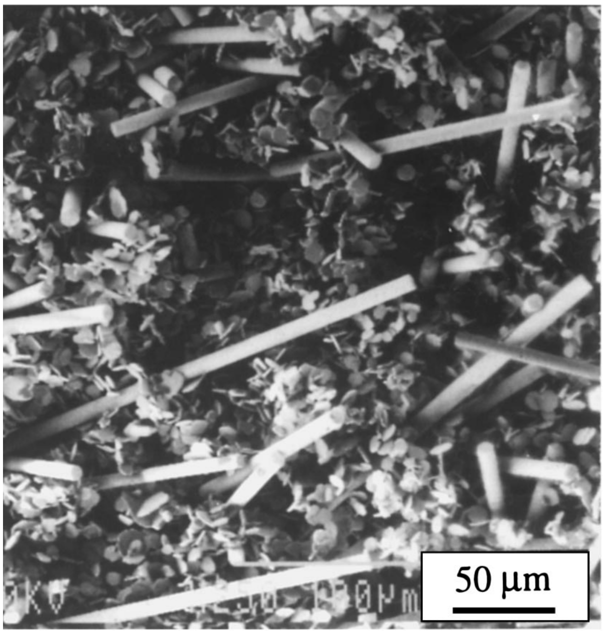

Figure 1 Microstructure of a hybrid preform, $r_f = 35\%$.

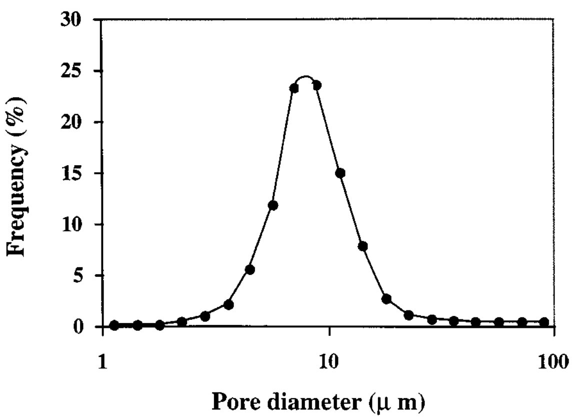

Figure 2 Pore volume histogram of a hybrid preform, $r_f = 35\%$.

and thus measure the work of fracture, it is necessary to notch the tensile specimens. The classical geometry (compact tension sample) was not successful and a planar crack was obtained with a specimen side notched on each face with a 0.3 mm saw and a razor blade (Fig. 3). We noticed that the width of the notch may have an effect on the measurement of the work of fracture. So, when the fiber percentage decreases ($r_f = 10\%$) it becomes necessary to reduce the notch width to 0.1 mm.

The specimens were loaded on an INSTRON machine with a 0.3 mm/min^{-1} crosshead speed so as to yield fully stable fractures. The displacement was measured using a LVDT transducer and the load applied with a 100 N cell.

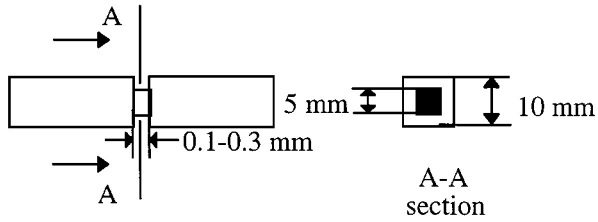

Figure 3 Specimen side notched on each face.

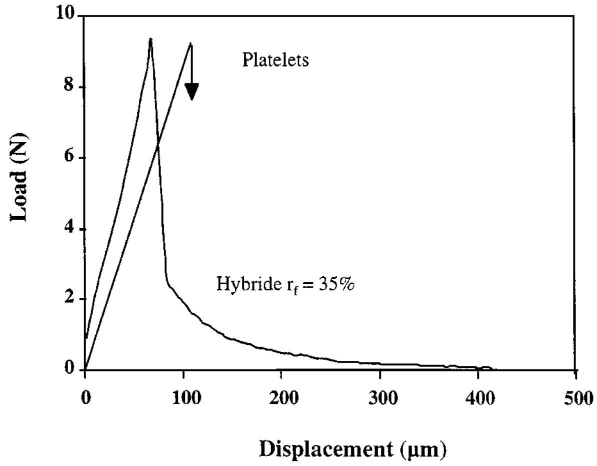

Figure 4 P–δ curves for platelets and 35% hybrid preforms.

4. Theoretical evaluation of the equivalent friction stress

Fig. 4 shows a typical P–δ curve obtained for $r_f = 35\%$ compared to the curve obtained with a preform containing only platelets. The curve corresponding to the preform without fibers exhibits a linear elastic increase up to the maximum load, followed by an abrupt load drop corresponding to a rapid propagation of the crack leading to the brittle failure of the specimen. On the contrary, three characteristic steps can be observed on the $P-\delta$ curve corresponding to $r_f = 35\%$: i) the same linear increase as previously described, ii) an abrupt load decrease ΔP corresponding to the rapid propagation of the crack in the section of the sample iii) a steady decrease of load corresponding to a controlled rupture of the sample, due to the pull-out process of crack-bridging fibers. The following parameters were derived from these curves:

—P_{max}, which is the maximum load
—γ, which is defined by the ratio $\Delta P/P_{max}$

To analyze quantitatively the effect of the introduction of fibers, we assume that these preforms are similar to a ceramic matrix composite, the 'matrix' being constituted by the platelet preform and the 'reinforcement' by the fibers. The total work of fracture W_{wof} for a steady state crack growth may be expressed by [7]:

$$W_{wof} = W_s + W_{pl} + W_d + W_p + W_r \qquad (1)$$

where W_s is the energy associated with the creation of new free surfaces, W_{pl} the matrix and the fibers plastic deformation energy, W_d the fiber–matrix debonding energy, W_p the fiber pull-out energy, and W_r the released relaxation energy of fibers.

Owing to the particular microstructure of the material, the bonds between platelets or between platelets and fibers occur only at particular points. So, when fracture of the platelet 'matrix' occurs, creating a planar rupture surface in this matrix, we can consider that the bonds between the fibers bridging the crack and the platelet 'matrix' are also broken. In this particular case, the energy W_0 given by the area under the linear part of the P–δ curve may be considered as including W_s and W_d. Moreover, due to the brittle nature of the materials, W_{pl} can be considered as negligible and the same conclusion seems to be valid for W_r, due to the very low value of stresses involved during the rupture of this kind of material. We can thus write:

$$W_{wof} \approx W_0 + W_p \quad (2)$$

W_p being represented by the area under the controlled rupture part of the load–displacement curve (Fig. 4).

In ceramic matrix composites, W_p is due to the friction between the debonded fibers and the matrix. In the case of our material, this friction is due to the local forces exerted between the platelets and the fibers through their contact. This force can be modeled by a uniform interfacial shear stress τ at the interface between the fibers and the matrix of the platelets.

With these simplifications, the models initially established for CMC could be used to determine an effective σ–δ traction law for the bridging fibers and the steady state bridging toughness increment W_p. The Jain model [8], is based on a number of assumptions, the following being easily transposable to our case: i) the matrix crack is planar and the fibers bridge this crack, ii) the fibers are straight with cylindrical geometry, inextensible and sufficiently strong to enable complete pull out without rupture, iii) the matrix deformation is negligible, iv) the strength distribution of fibers is rather narrow, v) it is the shorter embedded fiber segment bridging the matrix crack which will be pulled out. Moreover, it is also assumed in this model:

i) that the fiber embedded length l is less than the critical length $L_c = \sigma_f d_f / 4\tau$, where σ_f is the strength of the fibers of $2L_c$ gauge length, d_f their mean diameter and τ the interfacial shear stress. In the case of the materials studied, owing to the high porosity of the preform it can be assumed that τ is low. For example, if we take into account the other characteristics of the fibers and τ is of the order of 1 MPa, L_c should be more than one centimeter, which is much greater than the mean length of fibers.

ii) that a fiber with an orientation angle ψ to the pull-out load, suffers a bending in this direction (Fig. 5). To take this effect into account, the model introduces a snubbing friction coefficient f, correcting the load by a factor $e^{f\psi}$. The bending of the fiber, which may be envisaged for a bulk matrix, is less probable in the case of a porous material such as that studied here. We will thus assume no supplementary stress and take $f = 0$.

The load $P(\delta)$ corresponding to a crack opening δ may then be expressed by [8]:

$$P(\delta) = \sigma(\delta) \cdot S \text{ with } \sigma(\delta) = \frac{2\tau V_f}{d_f L_f} \cdot \delta^2 - \frac{2\tau V_f}{d_f} \cdot \delta + \frac{L_f \tau V_f}{2 d_f} \quad (3)$$

S being the section of the ligament, V_f the volume fraction of the fibers in the sample, L_f, d_f the mean length and mean diameter of fibers, and τ the equivalent interfacial shear stress defined above.

The extraction energy of fibers W_p is then given by:

$$W_p = \frac{\tau L_f^2 V_f}{12d} \qquad (\mathrm{J\,m^{-2}}) \quad (4)$$

5. Experimental results and interpretation

Table II gives P_{max}, γ, the displacement at rupture δ_r and the values of W_s, W_p and W_{wof} of the various preforms with the different weight fractions r_f of fibers. The volume fraction V_f of fibers in the preform is also given. In Fig. 6 the corresponding normalized load–displacement curves are plotted, with P/P_{max} as a function of δ.

The results show that the introduction of fibers increases the preform fracture toughness. This can be seen from the continuous increase of δ_r, W_p and of the ratio W_s/W_{wof} with r_f which is well illustrated by the relative disposition of the normalized curves of Fig. 6. The variations of W_s are more difficult to interpret, owing to the dispersion of results due to the crack tip effect. Indeed, the introduction of fibers decreases the cohesion of particles network and act as flaws. When the sample is notched, a rather large damage zone is created. It appears, however, that the total energy of rupture remains roughly constant for $r_f > 20\%$.

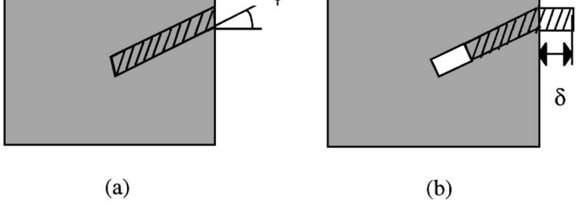

Figure 5 Pull-out of embedded fiber: (a) before loading, and (b) during pull-out.

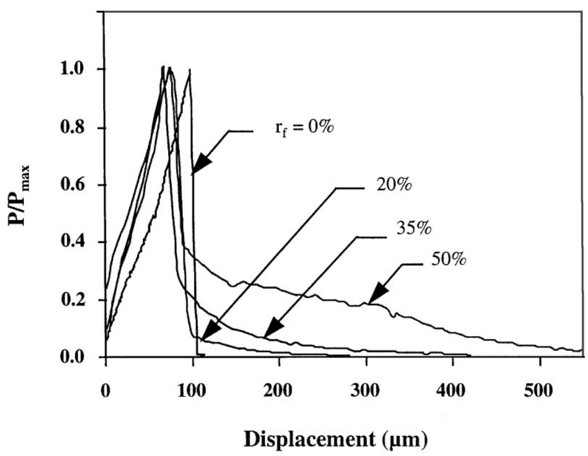

Figure 6 Load–displacement normalized curves for different fiber percentage.

TABLE II Mechanical characteristics of hybrid preforms

r_f (%)	V_f (%)	P_{max} (N)	γ	δ_r (μm)	W_s (J m^{-2})	W_p (J m^{-2})	W_{wof} (J m^{-2})	W_s/W_{wof}
0	0	9.2 ±0.2	1.0	109 ±1	19 ±1	0	19 ±1	1.00
10	2.2	9.2 ±0.5	0.6 ±0.1	210 ±20	14 ±3	5 ±1	19 ±4	0.74
20	4.3	13.2 ±2.2	0.8 ±0.1	285 ±15	27 ±9	6 ±1	33 ±10	0.82
35	7.5	9.5 ±2.0	0.6 ±0.2	440 ±50	16 ±8	15 ±5	31 ±13	0.52
50	10.5	7.8 ±0.5	0.7 ±0.1	480 ±100	11 ±3	18 ±6	29 ±9	0.38

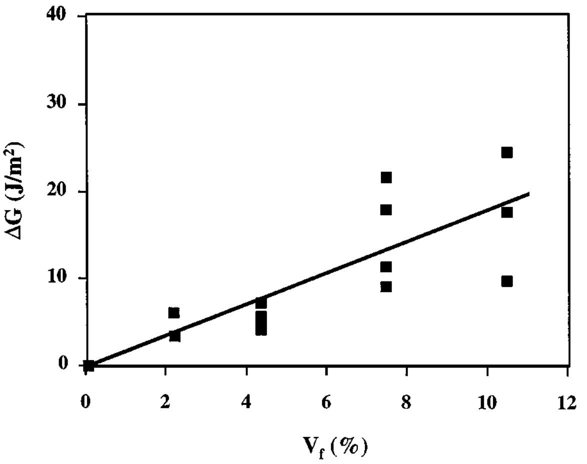

Figure 7 Fiber pull-out energy versus fiber volume fraction in the preform.

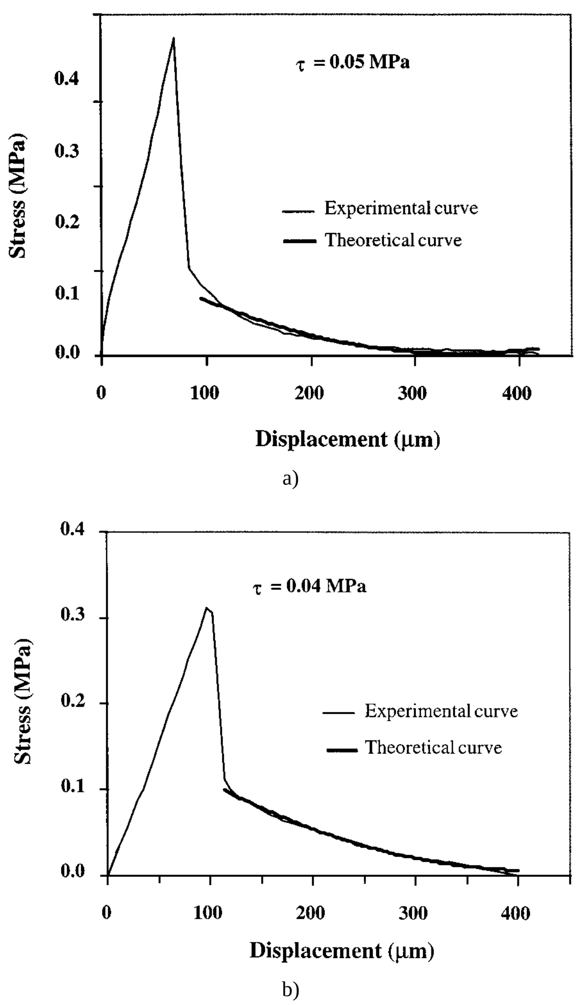

Figure 8 Example of τ determination by Equation 3: (a) $r_f = 35\%$ and (b) $r_f = 50\%$.

From these results, it is possible to evaluate the mean equivalent friction stress between the fibers and the platelets by means of Equation 4. The linear interpolation of the plot of W_p as a function of V_f (Fig. 7) leads to a τ value of 0.03 MPa. which corresponds to a maximum value of the order of 10^{-3} N for the force on each bridging fiber. This very low value is coherent with the physical origin of these forces.

Another evaluation of τ is possible from the P–δ curves by determining the τ value which leads to the best fit of the stage of the controlled crack opening by Equation 3. Fig. 8 gives two examples of the good fitting which can be obtained between experimental and theoretical curves for high r_f values (35% and 50%). Table III gives the mean values of τ determined by this method with the various preforms tested. For high r_f, τ values are found between 0.04 and 0.06 MPa, i.e. close to the value found previously by considering the evolution of W_d with V_f. However, determining τ by this method is difficult for low r_f values. In this case, the loads measured are very weak, especially in the final portion of the curve, which corresponds to the

TABLE III Mean τ values obtained from Equation 3

r_f (%)	10	20	35	50
τ (MPa)	0.29 ±0.01	0.07 ±0.02	0.06 ±0.02	0.04 ±0.01

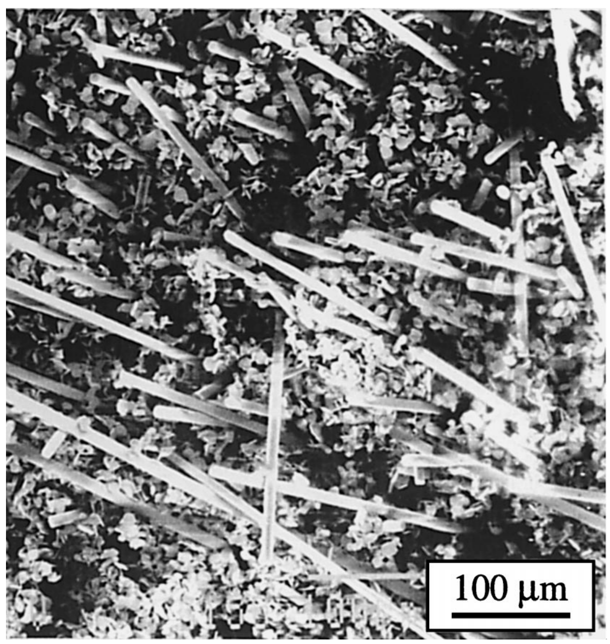

Figure 9 Fracture face of a hybrid preform showing pull-out ($r_f = 35\%$).

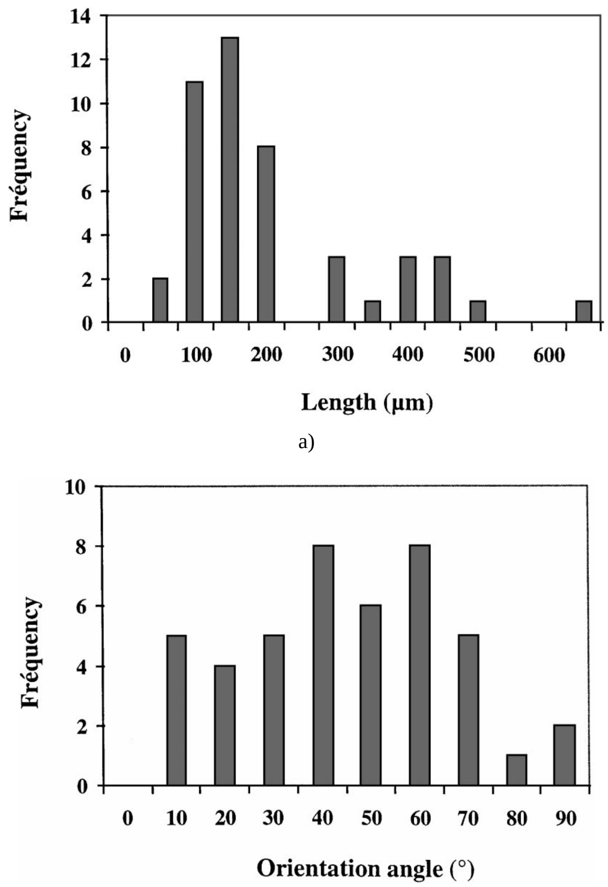

b)

Figure 10 Extracted fibers: (a) length distribution and (b) angle orientation distribution.

contribution of just a few fibers. The total extent of the stage of controlled crack opening is thus not correctly determined. This leads to a pseudo-load–displacement curve, the fitting of which gives incorrect τ values as can be seen for $r_f = 10\%$. It must be underlined that in this case, the estimation of τ according to Equation 4 should give much better results. Indeed the evaluation of the pull-out energy is much less sensitive to the exact determination of the end of the P–δ curve.

Observation of the fracture surfaces of a sample with $r_f = 35\%$ (Fig. 9) allowed us to check the validity of some hypotheses made on the material and on the pull-out process. The pull-out length and the angle ψ of the fibers with the fracture plane were determined by stereographic measurements on a population of 100 fibers. It can be seen in Fig. 10a that the ψ values are distributed rather homogeneously, which confirms the random orientation of fibers. The histogram of pull-out lengths (Fig. 10b) spreads from 0 to 500 μm (approximately $L_f/2$), with a maximum frequency of 150 μm. These values confirm the hypotheses made on the pull-out process: a variation of the fiber extracted length between 0 and $L_f/2$, no breakage of the fibers during the pull-out process, extraction of the shortest embedded length of a bridging fiber.

6. Conclusions

1) An experimental determination of the fracture energy of alumina preforms is possible, using quadruple notched specimens.

2) Platelet preforms exhibit a brittle fracture behavior. A hybridization of these preforms by short fibers leads to a change in this fracture behavior, which becomes partially controlled. This results in an increase in the work of fracture.

3) This work of fracture increase is due to the pull-out of the fibers bridging the crack. The models established in the case of CMC can be used to evaluate an equivalent friction stress on fibers, which is found to be of the order of 0.04 MPa for a preform with a total porosity of 80%.

References

1. V. MASSARDIER, R. FOUGERES and P. MERLE, *Mater. Sci. Eng.* A **203** (1995) 93.
2. V. MASSARDIER, R. FOUGERES and P. MERLE, *Mater. Sci. Eng. Lett.* A **185** (1994) 9.
3. S. V. KAMAT, A. D. ROLLET and J. P. HIRTH, *Scr. Metall.* **25** (1991) 27.
4. P. J. WHITERS, W. M. STOBBS and O. B. PEDERSEN, *Acta Metall.* **37** (1989) 2141.
5. R. HAMAN, P. F. GOBIN and R. FOUGERES, *Scr. Metall.* **24** (1990) 1789.
6. S. CARDINAL, PhD thesis, National Institute of Applied Sciences of Lyon (1997).
7. A. S. JAYATILAKA, *Fracture of Engineering Brittle Materials*, Londres (Applied Science publishers Ltd 1979) p. 256.
8. L. K. JAIN and R. C. WETHERHOLD, *Acta Metall.* **40** (1992) 1135.

Received 21 November 1997
and accepted 19 August 1998